

A measurement of the evolution of Interatomic Coulombic Decay in the time domain

F. Trinter¹, J. B. Williams¹, M. Weller¹, M. Waitz¹, M. Pitzer¹, J. Voigtsberger¹, C. Schober¹, G. Kastirke¹, C. Müller¹, C. Gohl¹, P. Burzynski¹, F. Wiegandt¹, T. Bauer¹, R. Wallauer¹, H. Sann¹, A. Kalinin¹, L. Ph. H. Schmidt¹, M. Schöffler¹, N. Sisourat², and T. Jahnke^{1*}

¹ *Institut für Kernphysik, Goethe Universität,
Max-von-Laue-Str.1, 60438 Frankfurt, Germany*

² *Université Pierre et Marie Curie, UMR 7614,
Laboratoire de Chimie Physique Matière et Rayonnement,
11 rue Pierre et Marie Curie, F-75005 Paris, France*

(Dated: September 17, 2018)

During the last 15 years a novel decay mechanism of excited atoms has been discovered and investigated. This so called "Interatomic Coulombic Decay" (ICD) involves the chemical environment of the electronically excited atom: the excitation energy is transferred (in many cases over long distances) to a neighbor of the initially excited particle usually ionizing that neighbor. It turned out that ICD is a very common decay route in nature as it occurs across van-der-Waals and hydrogen bonds. The time evolution of ICD is predicted to be highly complex, as its efficiency strongly depends on the distance of the atoms involved and this distance typically changes during the decay. Here we present the first direct measurement of the temporal evolution of ICD using a novel experimental approach.

In 1997 Cederbaum and coworkers realized that the presence of loosely bound atomic or molecular neighbors opens a new relaxation pathway to an electronically excited atom or molecule. In the decay mechanism they proposed - termed Intermolecular Coulombic Decay (ICD) - the excited particle relaxes efficiently by transferring its excitation energy to a neighboring atom or molecule [1]. As a consequence the atom or molecule receiving the energy emits an electron of low kinetic energy. The occurrence of ICD was proven in experiments in the mid 2000s by means of electron spectroscopy [2] and multi-coincidence techniques [3]. Since that time a wealth of experimental and theoretical studies have shown that ICD is a rather common decay path in nature, as it occurs almost everywhere in loosely bound matter. It has been proven to occur after a manifold of initial excitation schemes such as innervalence shell ionization, after Auger cascades [4, 5], resonant excitation [6, 7], shakeup ionization [8] and resonant Auger decay. ICD has also been observed in many systems as rare gas clusters [9], even on surfaces [10] and small water droplets [11, 12]. The latter suggested that ICD might play a role in radiation damage of living tissue [13], as it creates low energy electrons, which are known to be genotoxic [14, 15]. More recently that scenario was reversed as it was suggested to employ ICD in treatment of tagged malignant cells [16]. Apart from these potential applications the elementary process of ICD is under investigation, as the decay is predicted to have a highly complex temporal

behavior. The efficiency and thus the decay times of ICD depend strongly on the size of the system, i.e. the number of neighboring particles and the distance between them and the excited particle. However, even for most simple possible model systems consisting of only two atoms the temporal evolution of the decay is non-trivial and predicted theoretically to exhibit exciting physics [17]: as ICD happens on a timescale that is fast compared to relaxation via photon emission, but comparable to the typical times of nuclear motion in the system, the dynamics of the decay is complicated and so far only theoretically explored. As the decay rates strongly depend on the internuclear distances of the atoms participating in the decay the correct description of the nuclear motion as well as the precise decay widths for each distance are both vital even for predicting relatively general quantities, such as the energy spectrum of the emitted ICD electrons. Examining the temporal evolution of ICD in an experiment is therefore one of the grand challenges in ultrafast science. Here we present an experimental study resolving ICD in a helium molecule, a so called helium dimer (He_2), in the time domain.

The helium dimer is known to be the most weakly bound ground state system in the universe [18] with a binding energy of only 95 neV (1.1 mK) and a bond length that extends from about 5 Å over its mean value of 52 Å into the macroscopic regime of a few hundred angstroms. Nonetheless even in this extended system ICD occurs transferring about 40 eV of energy from one helium atom to its neighbor. The existence of ICD in the helium dimer has been shown in [19]. While initially ICD was investigated after innervalence ionization in the case of helium simultaneous photoionization and excita-

*Electronic address: jahnke@atom.uni-frankfurt.de

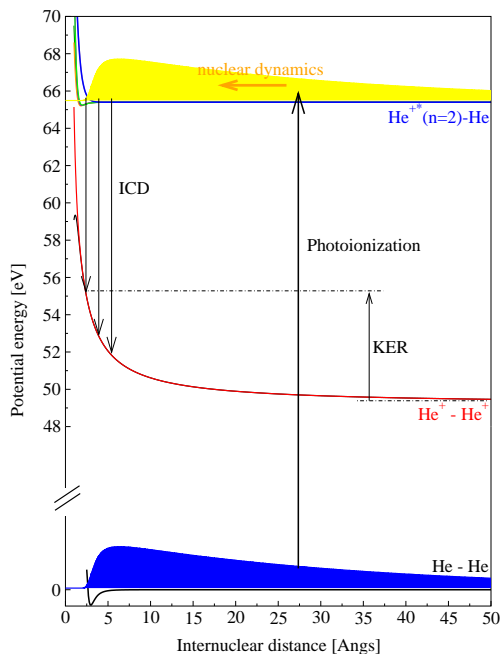


FIG. 1: Sketch of the potential energy diagram of the states involved in the process. The groundstate which is only bound by 95 neV is photoionized and excited. As the mean internuclear distance of the excited state is much smaller than that of the groundstate, nuclear motion sets in: the vibrational wavepacket starts to evolve on the potential energy curves of the excited states. During that time ICD happens mapping the evolving vibrational wavepacket to the repulsive He^+/He^+ final states. By measuring the kinetic energy release (KER) information on the internuclear distance (i.e. the distribution of the wavepacket) at the instant of the decay is obtained.

tion was used to produce an intermediate ionic dimer state that is able to undergo ICD. A multi-coincidence measurement yielded not only the proof of the existence of ICD even in a system as extended as the helium dimer, but for the first time showed the occurrence of nodal structures in the measured energy distributions [20]. Previously expected for the neon dimer [21] these occur as the vibrational wavefunction of the excited intermediate dimer state is mapped onto the repulsive final state after ICD visualizing directly the wave-nature of the vibrating nuclei. A sketch of the process and the involved potential energy curves is shown in Fig. 1. A key feature to ICD in He_2 is the long distance over which the energy transfer takes place. Consequently the decay times here are in comparison to that of other systems very long, allowing for the vibrational structure to form in the excited state. Following ICD in the time domain thus equals following the evolution of the vibrational wavepacket in time, as it is triggered at large internuclear distances and then evolves towards showing the vibrational features shown in Fig. 2.

We observe this time evolution, which takes place on a femto- to picosecond timescale making use of a new experimental technique, which maps time to kinetic energy of an emitted electron. Such a mapping of time to energy

is typically employed in attosecond science by streaking of electrons with a time varying external field [22]. In our novel technique the time dependent field is created by the decaying system itself and the photoelectron, which we launch in the pump step, acts as the probe particle, which experiences the streaking. In the present case we therefore used Cold Target Recoil Ion Momentum Spectroscopy (COLTRIMS) [23–25] to measure the energy of the photoelectron carrying the time information and the fragment ions on which we observe the time evolution of ICD in coincidence. By expanding helium gas at a pressure of 8 bar through a nozzle with a diameter of $5 \mu\text{m}$ and cooling the nozzle to a temperature of 22 K a supersonic gas jet containing a mixture of helium monomers and dimers was created. At these conditions a mixture of dimers and trimers might occur. The measurements, however, show that the contribution of trimers was small, as the measured spectra are expected to differ drastically for dimers and trimers. The supersonic jet was intersected by a linearly polarized photon beam with a photon energy of $h\nu = 65.536 \text{ eV}$ at beamline UE112-PGM-1 at the BESSY synchrotron facility. The ion detection covered full solid angle of emission for kinetic energy releases up to 3 eV. Ions with higher kinetic energy are detected depending on their emission angle, i.e. ions being emitted within a small cone along the spectrometer axis are detected over the complete range of KERs occurring in the reaction. These events have been used as a reference for a solid angle correction of the measured KER spectra.

Even though it is rarely stressed in literature, the mapping of decay time to photoelectron energy naturally occurs whenever a decay produces a secondary electron, which is significantly faster than the photoelectron [26, 27]. The change of the kinetic energy of the emitted particles is known as "post collision interaction" (PCI) [28]. So far, PCI has been studied in great detail after Auger decay [29]. As the Auger electron is emitted in the decay, the charge of the remaining ion changes. Accordingly an emerging photoelectron starts to leave a singly ionized atom, but as the decay happens, the photoelectron is suddenly exposed to the Coulomb force of a doubly charged ion. This results in lowering the energy of the emerging photoelectron and increasing the kinetic energy of the Auger electron. The energy shift of the photoelectron wavepacket depends on the time the Auger electron needs to emerge from the ion: a strong shift can be expected if the Auger electron is gone instantly, as the photoelectron is still close to the ion and the difference between the singly and the doubly charged potential is large in that case. The shift decreases for longer decay times correspondingly. Therefore, as the shift of the electron energy can be measured, a way to access the time domain of an electronic decay in an experiment arises. The only requirement for this scenario to work is, that the photoelectron is much slower than the secondary electron. Thus by tuning the photoelectron to very low energies the scheme can be used to measure the evolution of ICD. In order to convert the measured shift

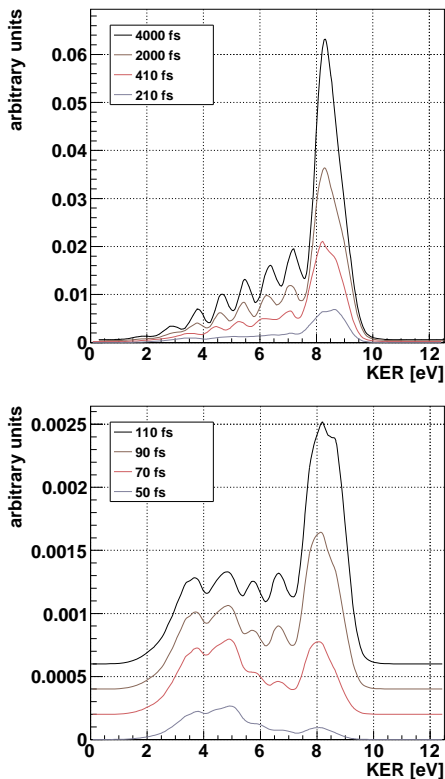


FIG. 2: Theoretical predictions of the time evolution of the kinetic energy release for different decay times. Bottom to top: KER for a time integrated from 0 fs to 50 fs, 70 fs, 90 fs, 110 fs, 210 fs, 410 fs, 2000 fs and to 4000 fs.

in energy of the photoelectron into a decay time we used a simple classical model. In a simulation an electron of a kinetic energy of 140 meV is launched. A second electron (the ICD electron) with a kinetic energy of 10 eV is launched after a delay time t_{ICD} . As the ICD electron reaches the photoelectron the distance the photoelectron travelled R_p is obtained. The energy difference between a Coulomb potential of charge two and a Coulomb potential of charge one at R_p is the amount of energy the electron is decelerated. This most simple model already shows a strong non-linear behavior for the dependency of the emission time of the second electron and the energy shift the first electron experiences as shown in Fig. 3 for different initial (i.e. unshifted) energies of the photoelectron. Apart from being a fully classical model it furthermore neglects effects that occur due to the different emission angles of the two electrons. However, this effect is known to be strong only for a small region of almost equal emission directions [30]. It furthermore turns out, that the minimum time that can be investigated depends on the initial energy of the photoelectron. This is basically due to the fact, that electrons that exhibit a severe shift are recaptured into the ion. Therefore, choosing an unperturbed energy of 140 meV for the photoelectron yields a minimum accessible decay time of 50 fs within our simple model. In the experiment this was implemented by employing a photon energy of 65.536 eV. At

this energy one helium atom of the dimer is ionized and excited to ($n=2$) and emits a photoelectron of an energy of 140 meV. This excited state can undergo ICD and was used (at higher photon energies) in the past to identify ICD in He_2 [19].

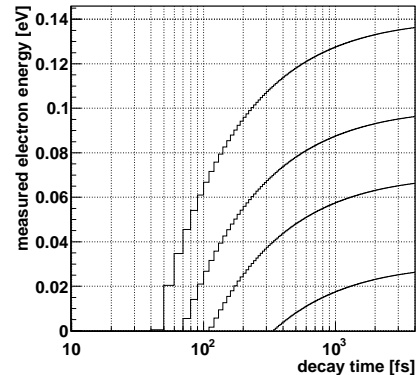


FIG. 3: Dependence of the shift in electron energy and the decay time obtained from our classical model. The plot depicts on the y-axis the energy a measured electron will have if the decay happens after a certain time (shown on the x-axis). The behavior is plotted for different initial photoelectron energies. From bottom to top: 30 meV, 70 meV, 100 meV, 140 meV.

In the present case the temporal evolution of the kinetic energy release (KER) is investigated. The KER is the energy that the two nuclei gain after dissociating in a Coulomb explosion as ICD occurred. The KER closely corresponds to the internuclear distance of the two atoms of the dimer, at the instant they were ionized: within the so called "reflection approximation" [31] the Coulomb interaction yields (in atomic units) the following simple relation: $\text{KER} = 1/R$. The results from the theoretical investigation shown in Fig. 2 depict the KER for different times at which ICD happened. At short times a first peak at lower kinetic energies occurs. This can be understood classically: as the internuclear distance of He_2 in the groundstate is much larger than in the excited state the decay starts to evolve at larger internuclear distances, i.e. smaller KERs. After some time the main peak at high KERs builds up as the dimer contracts towards the mean internuclear distance of the excited ionic state. As this happens, the probability for ICD increases (which is proportional to $1/R^6$ at large distances [32]) as Fig. 2 reveals. At longest times finally the vibrational features form, yielding the distribution, which is known from the non-timeresolved investigation [19, 20]. The time resolved KER spectra, shown in Fig. 2, were computed using the approach reported in [33]. The electronic structure input data used for these computations are presented and discussed in [34].

In Fig. 4 the experimental results are depicted. The top panel shows the correlation of the measured KER and the kinetic energy of the electrons. As expected the electron spectrum consists of a photoelectron line at an

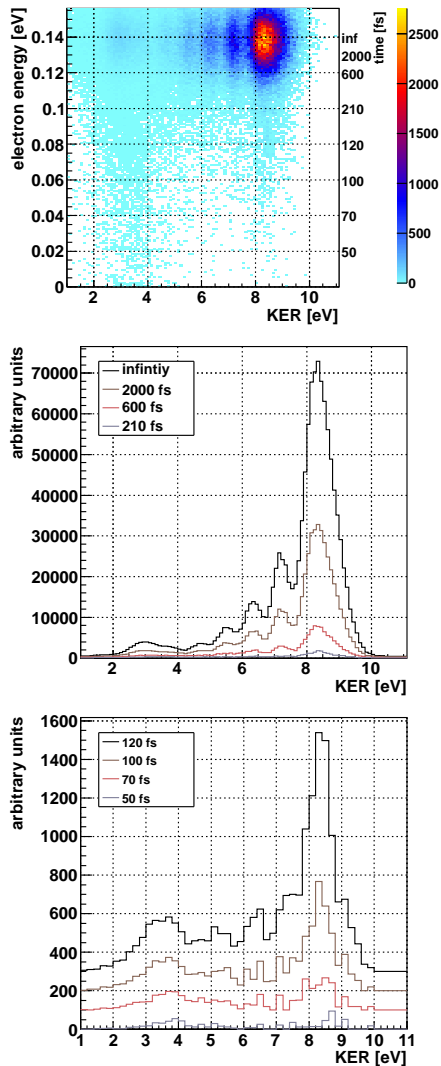


FIG. 4: Experimental results. Top: electron energies and kinetic energy releases measured in coincidence. The axis depicting the decay time is obtained according to our model described in the methods section. Middle and bottom: Measured kinetic energy releases corresponding to an integration over times from zero to (top to bottom): "infinity", 2000 fs, 600 fs, 210 fs, 120 fs, 100 fs, 70 fs, and 50 fs. The scaling of the y-axis is in both plots the same. All results shown here are solid angle corrected spectra (see methods for details), i.e. for KERs below 3.3 eV the y-axis shows counts, while the data with $\text{KER} > 3.3$ eV is multiplied by a KER dependent factor up to 9 for a KER of 12 eV.

energy of approx. 140 meV that is streaked towards lower electron energies. The plot reveals the expected behavior: at lowest photoelectron energies (which correspond to shortest ICD times) mainly low KERs occur. As the electron energy increases the main peak at a KER of about 8.5 eV builds up. For even later times the vibrational structures form. The two lower panels of Fig. 4 show the KER for different slices in the electron energy. The maximum photoelectron energy increases from bottom to top, accordingly the investigated time interval increases. The bottom panel shows the KER for electron energies of 0 meV to 20 meV, 40 meV, 60 meV, and 80 meV. The middle panel depicts KERs from 0 meV to 100 meV, 120 meV, 135 meV and 160 meV (full range), i.e. according to our model the time domain from 50 fs to "infinity". The experimental results furthermore confirm the findings of Fig. 2, that the decay times of ICD in He_2 are (due to the dimer's dimension) in the range of a few 100 femtoseconds to picoseconds, as the main contribution to the gathered data occurs at these times.

In conclusion we have added a new powerful streaking approach to the toolbox of ultrafast science and applied it to visualize the time dependence of an interatomic decay process. The results directly show the evolution of the vibrational wavepacket of a helium dimer during the decay and thus give insight into the complex behavior of ICD in the time domain. The measurement approach presented here can be used to investigate other processes and systems in the time domain, as well. Experiments investigating the evolution of a hole created inside an atom or molecule and for example the hopping of core holes in molecules could be traced in time in the future using the same approach.

I. ACKNOWLEDGMENTS

R.W. and T.J. would like to thank the Deutsche Forschungsgemeinschaft (DFG) for financial support. This research has been performed within the DFG-Forschergruppe FOR1789. We acknowledge the support from the staff at BESSY during the beamtime. We are indebted to R. Dörner for proposing this experiment.

-
- [1] L. S. Cederbaum, J. Zobeley, and F. Tarantelli. Giant intermolecular decay and fragmentation of clusters. *Phys. Rev. Lett.*, **79**, 4778 (1997).
 [2] S. Marburger, O. Kugeler, U. Hergenhahn, and T. Möller. Experimental evidence for Interatomic Coulombic decay in Ne clusters. *Phys. Rev. Lett.*, **90**, 203401 (2003).
 [3] T. Jahnke, A. Czasch, M. S. Schöffler, S. Schössler, A.

- Knapp, M. Kász, J. Titze, C. Wimmer, K. Kreidi, R. E. Grisenti, A. Staudte, O. Jagutzki, U. Hergenhahn, H. Schmidt-Böcking, and R. Dörner. Experimental Observation of Interatomic Coulombic Decay in Neon Dimers. *Phys. Rev. Lett.*, **93**, 163401 (2004).
 [4] Y. Morishita, X.-J. Liu, N. Saito, T. Lischke, M. Kato, G. Prümper, M. Oura, H. Yamaoka, Y. Tamenori, I.H.

- Suzuki, and K. Ueda. Experimental Evidence of Interatomic Coulombic Decay from the Auger Final States in Argon Dimers. *Phys. Rev. Lett.*, **96**, 243402 (2006).
- [5] K. Ueda, H. Fukuzawa, X.-J. Liu, K. Sakai, G. Prümper, Y. Morishita, N. Saito, I.H. Suzuki, K. Nagaya, H. Iwayama, M. Yao, K. Kreidi, M. Schöffler, T. Jahnke, S. Schössler, R. Dörner, Th. Weber, J. Harries, and Y. Tamenori. Interatomic Coulombic decay following the Auger decay: Experimental evidence in rare-gas dimers. *Journal of Electron Spectroscopy and Related Phenomena*, **3-10**, 166-167 (2008).
- [6] S. Barth, S. Joshi, S. Marburger, V. Ulrich, A. Lindblad, G. Öhrwall, O. Björneholm, and U. Hergenhahn. Observation of resonant Interatomic Coulombic Decay in Ne clusters. *J. Chem. Phys.*, **122**, 241102 (2005).
- [7] T. Aoto, K. Ito, Y. Hikosaka, E. Shigemasa, F. Penent, and P. Lablanquie. Properties of Resonant Interatomic Coulombic Decay in Ne dimers. *Phys. Rev. Lett.*, **97**, 243401 (2006).
- [8] T. Jahnke A. Czasch, M. Schöffler, S. Schössler, M. Kász, J. Titze, K. Kreidi, R. E. Grisenti, A. Staudte, O. Jagutzki, L. Ph. H. Schmidt, Th. Weber, H. Schmidt-Böcking, K. Ueda, and R. Dörner. Experimental Separation of Virtual Photon Exchange and Electron Transfer in Interatomic Coulombic Decay of Neon Dimers. *Phys. Rev. Lett.*, **99**, 153401 (2007).
- [9] G. Öhrwall, M. Tchapyguine, M. Lundwall, R. Feifel, H. Bergersen, T. Rander, A. Lindblad, J. Schulz, S. Peredkov, S. Barth, S. Marburger, U. Hergenhahn, S. Svensson, and O. Björneholm. Femtosecond Interatomic Coulombic Decay in Free Neon Clusters: Large Lifetime Differences between Surface and Bulk. *Phys. Rev. Lett.*, **93**, 173401 (2004).
- [10] G. A. Grieve, and T. M. Orlando. Intermolecular Coulomb Decay at Weakly Coupled Heterogeneous Interfaces. *Phys. Rev. Lett.*, **107**, 016104 (2011).
- [11] T. Jahnke, H. Sann, T. Havermeier, K. Kreidi, C. Stuck, M. Meckel, M. Schöffler, N. Neumann, R. Wallauer, S. Voss, A. Czasch, O. Jagutzki, A. Malakzadeh, F. Afaneh, Th. Weber, H. Schmidt-Böcking, and R. Dörner. Ultrafast Energy Transfer between Water Molecules. *Nature Physics*, **6**, 139 (2010).
- [12] M. Mücke, M. Braune, S. Barth, M. Förstel, T. Lischke, V. Ulrich, T. Arion, U. Becker, A. Bradshaw, and U. Hergenhahn. A hitherto unrecognized source of low-energy electrons in water. *Nature Physics*, **6**, 143 (2010).
- [13] H.-K. Kim, J. Titze, M. Schöffler, F. Trinter, M. Waitz, J. Voigtsberger, H. Sann, M. Meckel, C. Stuck, U. Lenz, M. Odenweller, N. Neumann, S. Schössler, K. Ullmann-Pfleger, B. Ulrich, R. Costa Fraga, N. Petridis, D. Metz, A. Jung, R. Grisenti, A. Czasch, O. Jagutzki, L. Schmidt, T. Jahnke, H. Schmidt-Böcking, and R. Dörner. Enhanced production of low energy electrons by alpha particle impact. *PNAS*, **108**, 11821 (2011).
- [14] B. Boudaiffa, P. Cloutier, D. Hunting, M. A. Huels, and L. Sanche. Resonant formation of DNA strand breaks by low-energy (3 to 20 eV) electrons. *SCIENCE*, **287**, 1658 (2000).
- [15] G. Hanel, G. Stier B., Denifl S., Scheier P., Probst M., Farizon B., Farizon M., Illenberger E., and Mark T. D. Electron attachment to uracil: Effective destruction at subexcitation energies. *Phys. Rev. Lett.*, **90**, 188104 (2003).
- [16] F. Trinter, M. S. Schöffler, H.-K. Kim, F. Sturm, K. Cole, N. Neumann, A. Vredenberg, J. Williams, I. Bocharova, R. Guillemin, M. Simon, A. Belkacem, A. L. Landers, Th. Weber, H. Schmidt-Böcking, R. Dörner, and T. Jahnke. Experimental Proof of Resonant Auger Decay Driven Intermolecular Coulombic Decay. *Nature, under consideration*, (2012).
- [17] A. I. Kuleff and L. S. Cederbaum. Tracing Ultrafast Interatomic Electronic Decay Processes in Real Time and Space. *Phys. Rev. Lett.*, **89**, 083201 (2007).
- [18] W. Schöllkopf, and J. Peter Toennies. Nondestructive Mass Selection of Small van der Waals Clusters. *SCIENCE*, **266**, 1345 (1994).
- [19] T. Havermeier, T. Jahnke, K. Kreidi, R. Wallauer, S. Voss, M. Schöffler, S. Schössler, L. Foucar, N. Neumann, J. Titze, H. Sann, M. Kühnel, J. Voigtsberger, J. H. Morilla, W. Schöllkopf, H. Schmidt-Böcking, R. E. Grisenti, and R. Dörner. Interatomic Coulombic Decay following Photoionization of the Helium Dimer: Observation of Vibrational Structure. *Phys. Rev. Lett.*, **104**, 133401 (2010).
- [20] N. Sisourat, Nikolai V. Kryzhevoi, P. Kolorenc, S. Scheit, T. Jahnke, and L. S. Cederbaum. Ultralong-range energy transfer by interatomic Coulombic decay in an extreme quantum system. *Nature Physics*, **6**, 508 (2010).
- [21] S. Scheit, L. S. Cederbaum, and H.-D. Meyer. Time-dependent interplay between electron emission and fragmentation in the interatomic Coulombic decay. *J. Chem. Phys.*, **118**, 2092 (2003).
- [22] M. Drescher, M. Hentschel, R. Kienberger, M. Uiberacker, V. Yakovlev, A. Scrinzi, Th. Westerwalbesloh, U. Kleineberg, U. Heinzmann, and F. Krausz. Time-resolved atomic inner-shell spectroscopy. *Nature*, **419**, 803 (2002).
- [23] R. Dörner, V. Mergel, O. Jagutzki, L. Spielberger, J. Ullrich, R. Moshhammer, and H. Schmidt-Böcking. Cold Target Recoil Ion Momentum Spectroscopy: a 'momentum microscope' to view atomic collision dynamics. *Physics Reports*, **330**, 96-192 (2000).
- [24] J. Ullrich, R. Moshhammer, A. Dorn, R. Dörner, L. Ph. H. Schmidt, and H. Schmidt-Böcking. Recoil-ion and electron momentum spectroscopy: reaction-microscopes. *Rep. Prog. Phys.*, **66**, 1463-1545 (2003).
- [25] T. Jahnke, Th. Weber, T. Osipov, A. L. Landers, O. Jagutzki, L. Ph. H. Schmidt, C. L. Cocke, M. H. Prior, H. Schmidt-Böcking, and R. Dörner. Multicoincidence studies of photo and Auger electrons from fixed-in-space molecules using the COLTRIMS technique. *J. Elec. Spec. Rel. Phen.*, **73**, 229-238 (2004).
- [26] B. Schütte, S. Bauch, U. Frühling, M. Wieland, M. Gensch, E. Plönjes, T. Gaumnitz, A. Azima, M. Bonitz, and M. Drescher. Evidence for Chirped Auger-Electron Emission. *Phys. Rev. Lett.*, **108**, 253003 (2012).
- [27] S. Bauch, and M. Bonitz. Theoretical description of field-assisted postcollision interaction in Auger decay of atoms. *Phys. Rev.*, **A85**, 053416 (2012).
- [28] A. Niehaus. Analysis of post-collision interactions in Auger processes following near-threshold inner-shell photoionization. *J. Phys.*, **B10**, 1845 (1977).
- [29] S. Sheinerman, P. Lablanquie, F. Penent, J. Palaudoux, J. H. D. Eland, T. Aoto, Y. Hikosaka, and K. Ito. Electron correlation in Xe 4d Auger decay studied by slow photoelectron-Auger electron coincidence spectroscopy. *J. Phys.*, **B39**, 1017 (2006).
- [30] A. L. Landers, F. Robicieux, T. Jahnke, M. Schöffler,

- T. Osipov, J. Titze, S.Y. Lee, H. Adaniya, M. Hertlein, P. Ranitovic, I. Bocharova, D. Akoury, A. Bhandary, Th. Weber, M. H. Prior, C. L. Cocke, R. Dörner, and A. Belkacem. Angular Correlation between Photoelectrons and Auger Electrons from K-Shell Ionization of Neon. *Phys. Rev. Lett.*, **102**, 223001 (2009).
- [31] E. A. Gislason. Series expansions for Franck-Condon factors. I. Linear potential and the reflection approximation. *J. Chem. Phys.*, **58**, 3702 (1973).
- [32] V. Averbukh, I.B. Müller, and L.S. Cederbaum. Mechanism of Interatomic Coulombic Decay in Clusters. *Phys. Rev. Lett.*, **93**, 263002 (2004).
- [33] Ying-Chih Chiang, Frank Otto, Hans-Dieter Meyer, and Lorenz S. Cederbaum. Interrelation between the Distributions of Kinetic Energy Release and Emitted Electron Energy following the Decay of Electronic States. *Phys. Rev. Lett.*, **107**, 173001 (2011).
- [34] P. Kolorenc, N. V. Kryzhevoi, N. Sisourat, and L. S. Cederbaum. Interatomic Coulombic decay in a He dimer: Ab initio potential-energy curves and decay widths. *Phys. Rev.*, **A82**, 013422 (2010).